Rapid-scanning terahertz precision spectrometer with more than 6 THz spectral coverage

G. Klatt,* R. Gebs, C. Janke, T. Dekorsy, and A. Bartels

Department of Physics and Center for Applied Photonics, University of Konstanz, D-78457, Germany
**Gregor.Klatt@uni-konstanz.de*

Abstract: We report a terahertz time-domain spectrometer with more than 6 THz spectral coverage and 1 GHz resolution based on high-speed asynchronous optical sampling. It operates at 2 kHz scan rate without mechanical delay stage. The frequency error of the system at 60 s acquisition time is determined by comparing a measured water vapor absorption spectrum to data reported in the HITRAN database. The mean error of 87 evaluated absorption lines is 142 MHz.

OCIS codes: (300.6495) spectroscopy, terahertz; (320.7150) ultrafast spectroscopy; (320.7090) ultrafast lasers.

References and links

1. M. Tonouchi, "Cutting-edge terahertz technology," Nat. Photonics **1**(2), 97–105 (2007).
2. D. Mittleman, *Sensing with terahertz radiation*, Springer series in optical sciences (Springer, 2003).
3. H. Harde, R. A. Cheville, and D. Grischkowsky, "Terahertz studies of collision-broadened rotational lines," J. Phys. Chem. A **101**(20), 3646–3660 (1997).
4. C. Fattinger, and D. Grischkowsky, "Terahertz beams," Appl. Phys. Lett. **54**(6), 490–492 (1989).
5. X.-C. Zhang, B. B. Hu, J. T. Darrow, and D. H. Auston, "Generation of femtosecond electromagnetic pulses from semiconductor surfaces," Appl. Phys. Lett. **56**(11), 1011–1013 (1990).
6. R. Huber, A. Brodschelm, F. Tauser, and A. Leitenstorfer, "Generation and field-resolved detection of femtosecond electromagnetic pulses tunable up to 41 THz," Appl. Phys. Lett. **76**(22), 3191–3193 (2000).
7. A. Sell, R. Scheu, A. Leitenstorfer, and R. Huber, "Field-resolved detection of phase-locked infrared transients from a compact Er:fiber system tunable between 55 and 107 THz," Appl. Phys. Lett. **93**(25), 251107 (2008).
8. G. Klatt, M. Nagel, T. Dekorsy, and A. Bartels, "Rapid and precise read-out of terahertz sensor by high-speed asynchronous optical sampling," Electron. Lett. **45**(6), 310–311 (2009).
9. S. Kim, B. Born, M. Havenith, and M. Gruebele, "Echtzeitnachweis von Änderungen im Protein-Wassernetzwerk während der Proteinfaltung mit Terahertz-Absorptionsspektroskopie," Angew. Chem. **120**(34), 6586–6589 (2008).
10. J. Wosnitza, A. Bianchi, J. Freudenberger, J. Haase, T. Herrmannsdörfer, N. Kozlova, L. Schultz, Y. Skourski, S. Zherlitsyn, and S. Zvyagin, "Dresden pulsed magnetic field facility," J. Magn. Magn. Mater. **310**(2), 2728–2730 (2007).
11. J. Xu, and X.-C. Zhang, "Circular involute stage," Opt. Lett. **29**(17), 2082–2084 (2004).
12. G.-J. Kim, S.-G. Jeon, J.-I. Kim, and Y.-S. Jin, "Terahertz Pulse Detection Using Rotary Optical Delay Line," Jpn. J. Appl. Phys. **46**(11), 7332–7335 (2007).
13. P. A. Elzinga, R. J. Kneisler, F. E. Lytle, Y. Jiang, G. B. King, and N. M. Laurendeau, "Pump/probe method for fast analysis of visible spectral signatures utilizing asynchronous optical sampling," Appl. Opt. **26**(19), 4303–4309 (1987).
14. A. Bartels, R. Cerna, C. Kistner, A. Thoma, F. Hudert, C. Janke, and T. Dekorsy, "Ultrafast time-domain spectroscopy based on high-speed asynchronous optical sampling," Rev. Sci. Instrum. **78**(3), 035107 (2007).
15. L. S. Rothman, C. P. Rinsland, A. Goldman, S. T. Massie, D. P. Edwards, J.- Flaud, A. Perrin, C. Camy-peyret, V. Dana, J. Y. Mandin, J. Schroeder, A. Mccann, R. R. Gamache, R. B. Wattson, K. Yoshino, K. V. Chance, K. W. Jucks, L. R. Brown, V. Nemtchinov, and P. Varanasi, "The HITRAN molecular spectroscopic database and HAWKS (HITRAN Atmospheric Workstation): 1996 edition," J. Quant. Spectrosc. Radiat. Transf. **60**(5), 665–710 (1998).
16. L. S. Rothman, I. Gordon, A. Barbe, D. Benner, P. Bernath, M. Birk, V. Boudon, L. Brown, A. Campargue, J.-P. Champion, K. Chance, L. Coudert, V. Dana, V. Devi, S. Fally, J.-M. Flaud, R. Gamache, A. Goldman, D. Jacquemart, I. Kleiner, N. Lacome, W. Lafferty, J.-Y. Mandin, S. Massie, S. Mikhailenko, C. Miller, N. Moazzen-Ahmadi, O. Naumenko, A. Nikitin, J. Orphal, V. Perevalov, A. Perrin, A. Predoi-Cross, C. Rinsland, M. Rotger, M. Simecková, M. Smith, K. Sung, S. Tashkun, J. Tennyson, R. Toth, A. Vandaele, and J. Vander Auwera, "The HITRAN 2008 molecular spectroscopic database," J. Quant. Spectrosc. Radiat. Transf. **110**(9-10), 533–572 (2009).
17. S. S. Harsha, N. Laman, and D. Grischkowsky, "High-Q terahertz Bragg resonances within a metal parallel plate waveguide," Appl. Phys. Lett. **94**(9), 091118 (2009).

#118303 - $15.00 USD Received 7 Oct 2009; revised 19 Nov 2009; accepted 20 Nov 2009; published 30 Nov 2009

18. R. Gebs, G. Klatt, H. Schafer, T. Dekorsy, and A. Bartels, Sub-100 fs time-domain spectroscopy using high-speed ASOPS, in *Lasers and Electro-Optics 2009 and the European Quantum Electronics Conference. CLEO Europe - EQEC 2009* (2009).
19. A. Leitenstorfer, S. Hunsche, J. Shah, M. C. Nuss, and W. H. Knox, "Detectors and sources for ultrabroadband electro-optic sampling: Experiment and theory," Appl. Phys. Lett. **74**(11), 1516–1518 (1999).
20. J. K. Wahlstrand, and R. Merlin, "Cherenkov radiation emitted by ultrafast laser pulses and the generation of coherent polaritons," Phys. Rev. B **68**(5), 054301 (2003).
21. R. Chakkittakandy, J. A. Corver, and P. C. Planken, "Quasi-near field terahertz generation and detection," Opt. Express **16**(17), 12794–12805 (2008).
22. A. Dreyhaupt, S. Winnerl, T. Dekorsy, and M. Helm, "High-intensity terahertz radiation from a microstructured large-area photoconductor," Appl. Phys. Lett. **86**(12), 121114–3 (2005).
23. D. L. Mills, and E. Burstein, "Polaritons: the electromagnetic modes of media," Rep. Prog. Phys. **37**(7), 817–926 (1974).
24. W. L. Faust, and C. H. Henry, "Mixing of Visible and Near-Resonance Infrared Light in GaP," Phys. Rev. Lett. **17**(25), 1265–1268 (1966).
25. S. Kasai, T. Katagiri, J. Takayanagi, K. Kawase, and T. Ouchi, "Reduction of phonon resonant terahertz wave absorption in photoconductive switches using epitaxial layer transfer," Appl. Phys. Lett. **94**(11), 113505 (2009).
26. M. Exter, C. Fattinger, and D. Grischkowsky, "Terahertz time-domain spectroscopy of water vapor," Opt. Lett. **14**(20), 1128–1130 (1989).

1. Introduction

In the past two decades terahertz time-domain spectroscopy (THz-TDS) has become an important tool for diverse applications in THz science and technology, including drug and food inspection, explosives detection, label-free DNA analysis or environmental gas analysis and sensing [1-3]. Well established techniques use ultrashort laser pulses from a modelocked laser for the generation and a delayed probe pulse for phase-sensitive detection of THz radiation. Such systems have been demonstrated covering a frequency range from a few tens of GHz well into the near infrared [4-7]. However, a significant disadvantage of common conventional systems employing linear mechanical delay stages to adjust the timing between the THz generation and detection pulses is the inherently low acquisition rate for THz transients. A 1 ns long THz transient, yielding the 1 GHz resolution typically needed to resolve spectral absorption features of environmental gases, requires a delay stage travel distance of 15 cm. The time required for accelerating and decelerating the stage between 10,000 or more data points and to efficiently average out technical laser noise leads to total acquisition times in the range of a few tens of minutes. This impedes applications where the acquisition of a THz trace must be completed within a few seconds or even milliseconds. Such applications include fast readout of resonant sensors [8], observation of structural dynamics in biomolecules [9] or experiments under rapidly varying environmental conditions, e.g. spectroscopy in high pulsed magnetic fields [10]. Faster mechanical approaches using rotating mirrors have been demonstrated with up to 400 Hz scan rate and up to 1 ns time delay [11,12]. While these present an important advance with respect to linear stages, two disadvantages remain: a) mechanical masses rotating at >10,000 rpm on an optical table are a significant noise source and b) to effectively avoid laser noise with typical Fourier content up to 1 kHz, the demonstrated scan rates for rotary stages are yet too low. Furthermore, all mechanical delay stages are susceptible to calibration errors of amplitude and time-delay due to alignment errors and manufacturing tolerances.

Asynchronous optical sampling (ASOPS) is a time-domain spectroscopy technique first introduced with picosecond lasers in the late eighties that employs no mechanical delay stage and thus eliminates the problems outlined above [13]. A recently introduced high-speed implementation of ASOPS uses two Ti:sapphire femtosecond lasers whose repetition rates of 1 GHz are linked with an offset Δf_R of a few kilohertz [14]. As a result of the offset, the delay between pairs of pulses from the lasers is repetitively ramped between zero and the inverse laser repetition rate at a scan rate equal to Δf_R. The key advantage of high-speed ASOPS lies in the scan rates of several kilohertz, a performance that is impossible with conventional systems. It allows completing the acquisition of a time-domain trace before technical noise of common femtosecond lasers with significant Fourier content in the acoustic regime up to 1 kHz can affect the signal. This permits measurements at the shot-noise limit without the use of lock-in amplifiers or other noise suppression measures.

#118303 - $15.00 USD Received 7 Oct 2009; revised 19 Nov 2009; accepted 20 Nov 2009; published 30 Nov 2009

To realize a THz-TDS system, one laser is used to generate the THz radiation, the second laser is used to detect the THz waveform in the same detection geometry as in a conventional THz-TDS setup [4-7]. The THz waveform is mapped onto the intensity of the detection laser beam which is measured and digitized as a function of real-time t and recalibrated to a time-delay scale τ using a factor $\Delta f_R/f_R$, where f_R is the repetition rate of the THz generation laser. High-speed ASOPS has been realized with a time resolution of 160 fs, limited by timing jitter between the offset-locked lasers, and has enabled THz-TDS at 1 GHz resolution and 10 kHz scan rate without mechanical delay stage at a spectral coverage of 3 THz [14]. In this letter we report a high-speed ASOPS based THz-TDS system with a significantly enhanced time resolution of 40 fs, now determined by the laser pulse duration, leading to a spectral coverage of more than 6 THz. To assess the utility of the system for rapid and precise spectroscopy, we have carefully compared a measured water vapor absorption spectrum to data reported in the HITRAN database [15,16] and find a mean frequency deviation of 142 MHz and a maximum deviation of 461 MHz at 60 s acquisition time. While frequency *repeatability* tests have been reported previously [8,17], our experiment is - to the best of our knowledge - the first systematic *accuracy* evaluation of a THz-TDS system.

2. Experimental setup

The laser system and optical setup are equivalent to a previously reported system with f_R = 1 GHz that was offset-locked at the third repetition rate harmonic with Δf_R = 10 kHz [14]. However, we have implemented four major improvements to enhance the bandwidth performance. (a) The phase-locked loop electronics used to offset-stabilize the two lasers in a master-slave configuration now operate at the tenth harmonic of the repetition frequency. Due to the resulting enhanced phase-noise sensitivity, the feedback loop is able to perform a tighter offset lock with reduced timing jitter. At the same time, the frequency shifter previously used to define the offset frequency has been replaced by direct-digital synthesis electronics allowing for a better calibration of the experimental time-delay axis [18]. (b) The repetition rate difference is reduced to 2 kHz, a value that was previously impossible to attain due to adverse effects of sidebands generated in the frequency shifter employed to define the repetition rate offset [14]. The reduced repetition rate difference in combination with the 1 GHz repetition rate and the 100 MHz detector and A/D-converter bandwidth yields an enhanced data point density of one point every 20 fs, supporting the time-resolution enabled by the 40 fs laser pulses. (c) The trigger signal for the data acquisition is generated optically via two-photon absorption in a GaP photodiode instead of electronically via mixing of electronic signals at the repetition rates. This eliminates slow drifts on the order of 100-200 fs that previously occurred between the THz signal and the trigger signal. (d) The ZnTe crystal used for electro-optic detection via the Pockels effect was replaced because of the crystal's reststrahlen band between 5.3 THz and 6.1 THz. Instead a 400 µm thick (110)-GaP crystal was used whose TO phonon frequency lies at 11 THz, safely beyond the bandwidth expected for our setup due to the 40 fs duration of the laser pulses [19-21].

3. Results and discussion

Figure 1 shows the first 35 ps of a 1 ns long THz transient obtained with the spectrometer under purging with dry air and with 9 minutes data acquisition time. The main THz pulse is generated by an optical pump pulse of 40 fs duration and 55 µm spot size (FWHM) with an average power of 550 mW in a large area photoconductive THz emitter. The emitter is biased with 10 V which corresponds to an electric field of 20 kV/cm for the acceleration of electrons. Details of the emitter are described elsewhere [22]. The satellite signals at 9 ps and 16 ps and combinations of these values at later time-delays result from internal reflections of the main THz pulse in the 400 µm thick GaP detector crystal and in the 645 µm thick GaAs emitter substrate, respectively. The inset of Fig. 1 shows the corresponding Fourier transform of the full time-domain data. The modulation arises from the multiple reflections of the main THz pulse. The spectral coverage above the noise floor ranges from 0.2 to 6.5 THz.

#118303 - $15.00 USD Received 7 Oct 2009; revised 19 Nov 2009; accepted 20 Nov 2009; published 30 Nov 2009

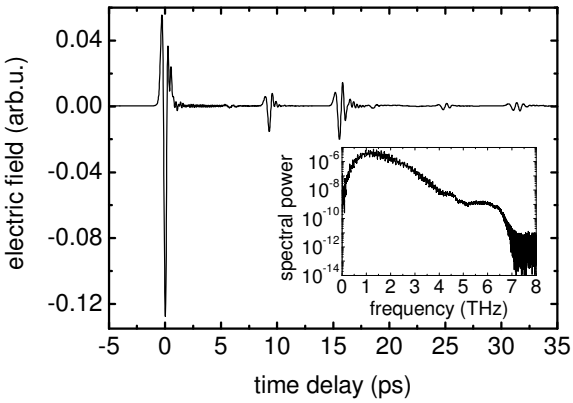

Fig. 1. Transient with multiple reflections of the THz pulse in the THz emitter substrate and GaP detection crystal. The inset shows the corresponding Fourier transform.

Fast oscillations present on the signal after the main THz pulse (Fig. 2 (a)) arise from the propagation of phonon-polaritons in the GaAs emitter substrate [20,23]. The phonon-polariton dispersion is given by

$$\omega = ck / \sqrt{\varepsilon(\omega)}\,, \tag{1}$$

where $\varepsilon(\omega)$ is the dielectric function of a diatomic cubic lattice without damping, ω the angular frequency, k is the coupled mode wavevector and c the vacuum light speed.

The phonon-polariton dispersion leads to a delay of the higher frequency components close to ω_{TO} upon propagation through the emitter substrate, which is directly observable in the time-domain trace. To point this further out, Fig. 2 (b) shows a Fourier transformation of the time-domain trace after the main pulse. A Fourier transform window of 1 ps length is swept over the trace to obtain the 2D plot. All frequencies above 4.5 THz are delayed, the maximal observed time delay is 10 ps. The additional pulses in Fig. 2 (b) at 6 and 9 ps arise again from internal reflections of the THz main and the probe pulse in the emitter and detector substrates. For comparison, the analytical dispersion relation is used to generate a 2D plot of the delayed frequency components (Fig. 2 (c)). The calculated spectrum does not include lattice damping of the phonon-polariton, which causes the broadening of the spectrum at larger time delays. Apart from this and the fact that the calculation omits the additional maxima at 6 and 9 ps the calculated plot shows a good agreement with the experimental data.

The spectral coverage of the spectrometer is limited to 7 THz due to the nonlinear response function of the GaP detection crystal. In the THz frequency range an electronic part as well as an ionic part contributes to the second order susceptibility χ^2. The ratio between both parts is described by the Faust-Henry coefficient [24]. For many semiconductors such as GaP the Faust-Henry coefficient is negative describing the fact that the contributions subtract from each other for frequencies below the TO phonon frequency. In the case of GaP, both contributions cancel out in the frequency range around 7 THz [19,20,24]. While the response of GaP recovers beyond the minimum around 7 THz, in the current configuration the spectrometer is still limited to frequencies below 8 THz due to the TO phonon of the GaAs emitter substrate. This problem could be solved by either using the emitter in reflection geometry or by thinning down the emitter substrate [25]. Beyond 8 THz, the 40 fs pulse length of the 1 GHz Ti:sapphire lasers would limit the spectral coverage.

#118303 - $15.00 USD Received 7 Oct 2009; revised 19 Nov 2009; accepted 20 Nov 2009; published 30 Nov 2009

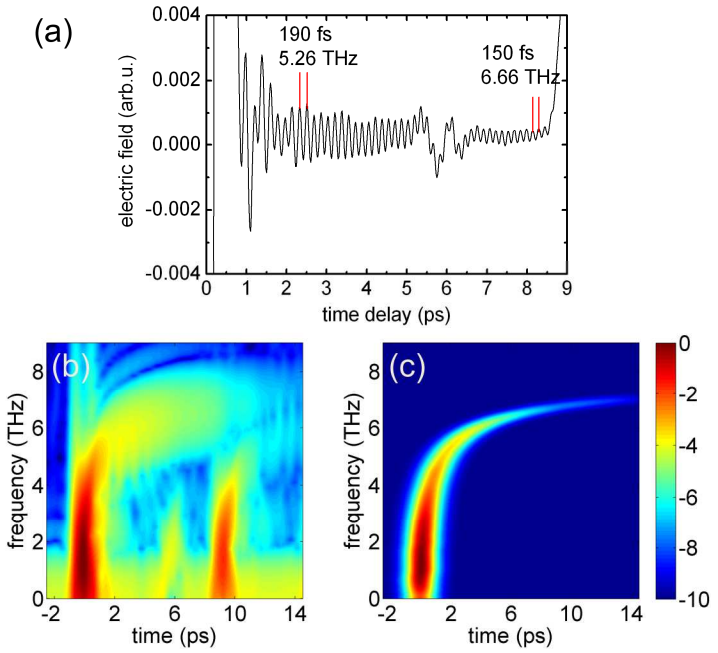

Fig. 2. (a) Zoom-in into the first picoseconds after the main THz pulse. The larger delay of higher frequency components is readily visible in the time-domain. (b) FFT with a sweeping time window of 1 ps length of the time-domain data shown in (a). (c) Corresponding calculated 2D plot of the delayed frequency components, generated from the phonon-polariton dispersion relation. The color of both 2D plots maps the FFT intensity onto a logarithmic scale.

The frequency accuracy of a THz-TDS system is determined by the factors influencing the accuracy of the time-delay scale τ. For a conventional THz-TDS system this is entirely given by the calibration of the delay stage and its alignment. In a high-speed ASOPS based system the time-delay is given as $\tau = t \times \Delta f_R / f_R$ and its accuracy is thus determined by that of the spectrum analyzer or frequency counter used to measure the repetition rates and the system clock of the A/D converter that defines the real-time scale t. In principle, these instruments can be provided with frequency references with an accuracy that can be as good as that of a cesium atomic clock (10^{-15}) or a more readily available commercial GPS-referenced Rubidium reference (10^{-12}). Here, however, we have used a lower cost oven stabilized crystal oscillator with a relative frequency uncertainty of approximately 10^{-7}. Another factor influencing the accuracy of a high-speed ASOPS based system are fast systematic deviations of the true $\Delta f_R/f_R$ value from the nominal value that occur during a measurement cycle and are in phase with the trigger signal, i.e. they repeat for each measurement and thus persist despite averaging. These systematic deviations can be caused by modulations of Δf_R due to imperfections in the offset-locking electronics. Using a cross-correlation technique, we have found that the mean relative deviation of $\Delta f_R/f_R$ from the nominal value is 9.8×10^{-5}, the maximum relative deviation of the frequency calibration is 1.7×10^{-4} [18].

To test the spectral accuracy of our THz-TDS system, atmospheric water vapor is one of the samples best suited [26]. Between 0.2 and 6.5 THz more than 1000 absorption lines are well known from experimental and theoretical investigations and are documented in the HITRAN database [15,16]. The reported frequency error of the HITRAN data for water vapor is between 300 kHz and 3 MHz, enabling us to test our system at this accuracy level. The width of each absorption line at atmospheric conditions lies in the range of 10 GHz. This is well-matched to the 1 GHz resolution of our THz-TDS system determined by the 1 ns observation window. Figure 3 shows the comparison between a measured and calculated water vapor absorption spectrum. The acquisition time for the trace with water vapor was

#118303 - $15.00 USD Received 7 Oct 2009; revised 19 Nov 2009; accepted 20 Nov 2009; published 30 Nov 2009

60 s, the reference data are the 9-minute data shown in Fig. 1. The data for the calculation are taken from the latest version of the HITRAN database [16] and the calculation is carried out according to the formulas of reference [15]. During the 60 s measurement the ambient parameters were kept constant (temperature 20°C, pressure 1015 hPa, relative humidity 26%).

Up to a frequency of 2.5 THz the line positions as well as the line strength agree very well. For greater frequencies absorption measurements are limited by the dynamic range of the spectrometer. Lines with an absorption higher than 0.15 cm^{-1} cannot be fully resolved (see inset Fig. 3).

For a more accurate analysis of the water vapor absorption data, all measured absorption lines from 0.2 to 6.5 THz were fitted with Lorentz line shape functions given by

$$\alpha(\nu) = S \cdot \rho \cdot \frac{1}{\pi} \cdot \frac{\gamma}{\gamma^2 + (\nu - \nu_0)^2}, \qquad (2)$$

where α is the absorption coefficient in cm^{-1}, ν the wavenumber in cm^{-1}, S the line intensity in cm^{-1}/(molecule * cm^{-2}), ρ the number of H_2O molecules per cm^3, γ the pressure dependent half width (HWHM) in cm^{-1} and ν_0 the pressure corrected line position in cm^{-1}. For more details see reference [15]. The experimental data were evaluated by an automatic numerical routine, which extracts all line positions and performs a Lorentz line shape fit for every found absorption line. For all noisy lines - lines with > 2.5 THz and > 0.15 cm^{-1} - the noisy part is deleted by the routine before performing the fit.

In the range from 0.2 to 6.5 THz there are 147 lines with an intensity greater than 3×10^{-21} cm^{-1}/(molecule * cm^{-2}). This intensity is the lower detection limit of the spectrometer in the range from 0.2 to 6.5 THz. 87 lines are evaluated by the automated numerical routine. The other 60 lines are either too close to at least one other line and lead to non-converging fits, or their intensity is too weak to detect them numerically. The mean deviation of the line positions ν_0 from the HITRAN data over all fitted lines is 142 MHz. The mean relative deviation is 5.7×10^{-5}. The largest deviation of any line is 461 MHz, corresponding to a relative deviation of 2.5×10^{-4}. These errors are consistent with the above estimated effect of a systematic miscalibration of the time-delay versus real-time scale due to imperfections in the locking electronics. The errors of our measurements of temperature (± 1K), pressure (± 5hPa), and humidity (± 2% relative humidity) cause only negligible uncertainty (maximum ± 1.5 MHz) in the calculation of the ν_0 from the HITRAN database and are not significant in the evaluation of the frequency error.

The averaged relative deviation of the line intensity S from the calculated spectrum based on the HITRAN data is 6.0% for the fully resolved lines below 2.5 THz and increases to 12.3% when all evaluated lines are considered. This is consistent with the 6% uncertainty in the calculated line intensity due to the mentioned errors of temperature, pressure and humidity and additional errors expected from the limited dynamic range of the spectrometer above 2.5 THz.

We have repeated the same evaluation for data acquired with 0.6 s acquisition time. The mean and maximum deviations from the HITRAN database increase only slightly to 164 MHz and 468 MHz, respectively. While these values are similar to the data at 60 s acquisition time, the available spectral coverage was reduced to 3.5 THz due to a reduced signal-to-noise ratio above this value.

#118303 - $15.00 USD Received 7 Oct 2009; revised 19 Nov 2009; accepted 20 Nov 2009; published 30 Nov 2009

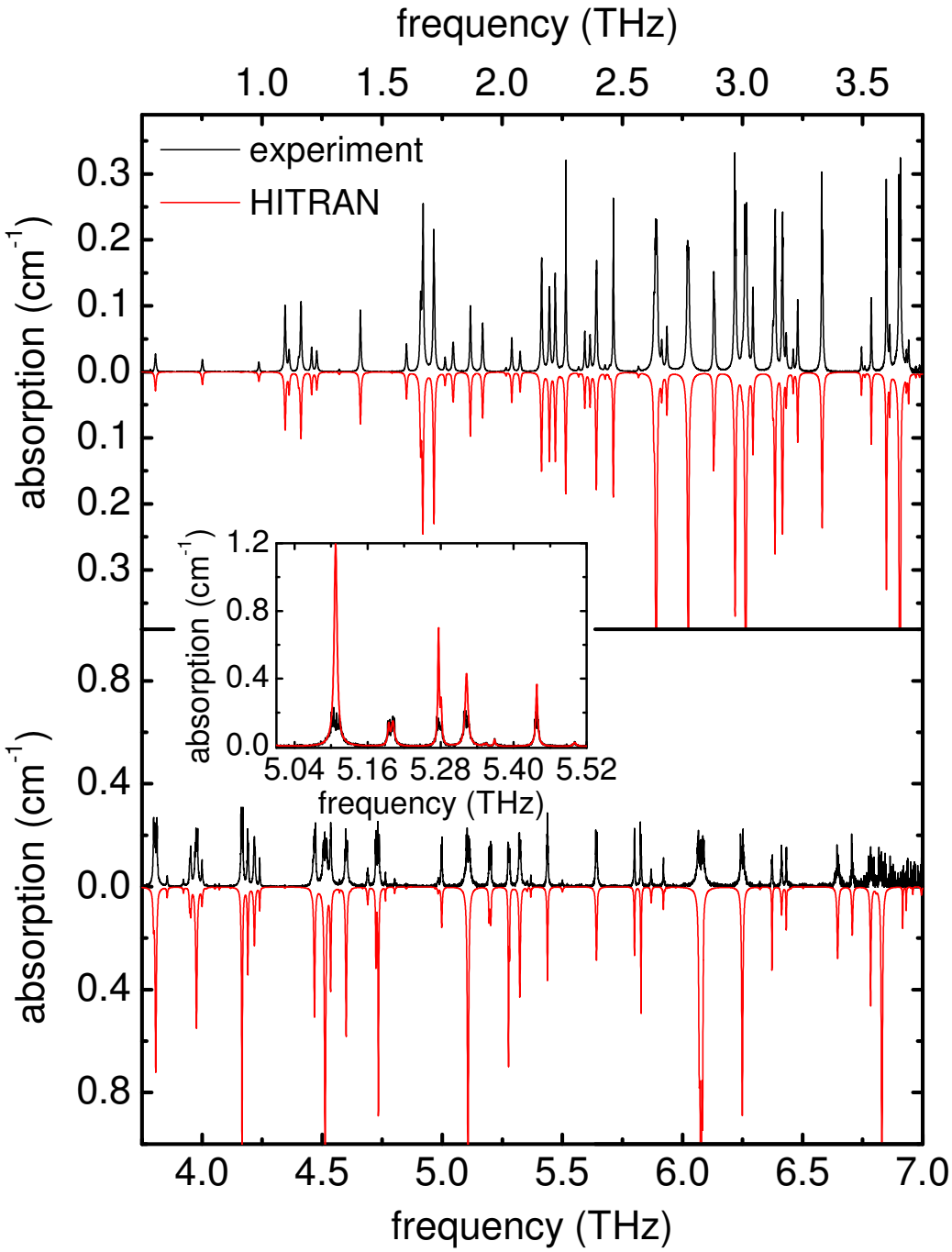

Fig. 3. Measured (black) and calculated (red) absorption spectra of water vapor. The inset shows a detailed view of the absorption spectra around 5.28 THz.

4. Conclusion

In conclusion we have demonstrated a high-speed ASOPS based THz-TDS spectrometer operating without mechanical delay at 2 kHz scan rate. The instrument offers a unique combination of more than 6 THz spectral coverage and 1 GHz spectral resolution. The

#118303 - $15.00 USD Received 7 Oct 2009; revised 19 Nov 2009; accepted 20 Nov 2009; published 30 Nov 2009

precision of the spectrometer has been evaluated relative to water vapor absorption data published in the HITRAN database. The mean deviation for the line positions is 142 MHz and the maximum deviation is 461 MHz at an acquisition time of 60 s and only slightly larger at 0.6 s acquisition time. Our instrument should be particularly useful for applications where rapid data acquisition in combination with a high frequency accuracy and high resolution is important.

Acknowledgments

We thank A. Leitenstorfer for helpful discussions. This research is supported by the Landesstiftung Baden-Württemberg. This work is partially supported by the Ministry of Science, Research and the Arts of Baden-Württemberg and the Deutsche Forschungsgemeinschaft.

#118303 - $15.00 USD Received 7 Oct 2009; revised 19 Nov 2009; accepted 20 Nov 2009; published 30 Nov 2009